Potential anti-inflammatory effects of Pingyin Rose Essential Oil on Lipopolysaccharide-induced HaCaT Cells

Jingyi Song
Beijing Technology and Business University
Rifat Nowshin Raka
Beijing Technology and Business University
Yue Yuan
Beijing Technology and Business University
Suyeon Park
Beijing Technology and Business University
Juan Wang
Beijing Technology and Business University
Fei Liu
Shangdong Freda Biotech Co., Ltd
Hua Wu (wuhua@btbu.edu.cn)
Beijing Technology and Business University
Junsong Xiao
Beijing Technology and Business University
Mingquan Huang
Beijing Technology and Business University
Suzhen Yang
Shangdong Freda Biotech Co., Ltd

Research Article

Keywords: Inflammation, Pingyin rose essential oil, NF-kappa B, Toll like receptor 4, Oxidative stress, HaCaT cell, Ectopic olfactory receptors

Posted Date: March 1st, 2022

DOI: https://doi.org/10.21203/rs.3.rs-1326521/v1

Abstract

Background: Skin is the primary defense to human body from external exposure of harmful stimulation. Excessive and improper immune-regulation could cause chronic inflammation resulting in different skin diseases. Pingyin Rose is a well-known component of traditional Chinese medicine (TCM) because of its wide range of bioactivities and so do PREO.

Aim: The present work aims to characterize the Pingyin rose essential oil (PREO) composition, investigate the beneficial effects of PREO on the skin inflammation *in vitro* and determine ligands for OR2AT4 *in silico* from PREO components.

Materials and Methods: PREO was quantified by GC-MS and molecular docking was performed for OR2AT4 with top two components. HaCaT cells were induced with lipopolysaccharides (LPS) to study downregulation of oxidative stress and inflammation through NF-κB signaling.

Result and Discussion: According to our results, Citronellal (54.28%) and geraniol (9.26%) are the principal compounds of PREO and both deemed to be potential ligand for OR2AT4. PREO could significantly reduce the expression of the TLR4-NF-κB pathway in LPS-induced HaCaT cells. PREO could also prevent LPS-mediated oxidative stress, including the increase of SOD and MDA, decrease of mRNA expression for inflammatory markers (TNF-α, IL-1β, IL-6, IL-8) and several genes involved in TLR4 pathway, that is also an evident for PREO as potential anti-inflammatory therapeutic. PREO also inhibits NF-κB p65 and IκB-α protein phosphorylation.

Conclusion: Our findings revealed that PREO could decrease inflammatory protein expressions, possibly functioning with the reduction of oxidative stress and inflammatory cytokines via downregulating NF-κB pathway. PREO component can interact with OR2AT4 and paly roles in other physiological activities.

1. Background

Epidermal inflammation is the main cause of skin health impairment. Being the interface between the body and the outside environment, skin must deal with external harmful stimuli including pathogenic microorganism invasion, stress, radiation etc. [1]. Generally, there is a balance between pro- and anti-inflammatory cytokines in healthy body, but the overproduction of pro-inflammatory mediators will break the equilibrium and cause oxidative reactions [2]. This phenomenon causes skin lesions and eventually leads to epidermal inflammation. Overproduction of inflammatory mediators such as tumor necrosis factor alpha (TNF-α), interleukins (IL-1, IL-6, IL-10), nitric oxide (NO) and reactive oxygen (ROS) secreted by local cells play a key role in this imbalance [3]. This is the reasons of follicular epithelium damage and melanin deposition induction [4]. However, the underlying signaling pathway of skin inflammation is complex and need to be explored. Now, there are many types of anti-inflammatory medications available on the market like NSAIDs and antibiotics. However, these drugs have side effects and in the course of time, they develop resistance [1, 5]. Therefore, it is a smart choice to search for an alternative solution from traditional medicine.

Traditional Chinese Medicine (TCM) has a long history of anti-inflammatory medication that includes a variety of natural compounds. As skin inflammation is susceptible to frequent exposure to harmful stimulators, suppressing inflammatory pathways and neutralizing oxidation are promising approaches to treat inflammation [6–9] Pingyin Rose, especially it's flower bud, is a well-represented component of TCM for its fragrance and therapeutic efficacy. It is natively cultivated in Pingyin town; Shandong province aliased as the "Second Land of Rose" in China. There are different scientific evidences proving different bioactivities of *Rosa rugosa* [10–12].Pingyin rose essential oil (PREO) extracted from *Rosa rugosa cv. Plena* that is a popular cosmetic additive (Chinese Materia Medica, 1998; TCM Wiki. Retrieved 5, February 2017). Terpenes are present in decent amount in PREO and individually these components have shown anti-inflammatory effects in different studies (Tung et al.2008; Borges et al. 2019). Local medicine practitioner found that PREO has some activities like anti-inflammatory, anti-oxidation, and anti-anxiety etc. However, there is little experimental verification to that [13–15]

As a composition of odorant molecule, PREO is likely to bind with ectopic olfactory receptors (EORs). OR2AT4 is a skin EOR which takes part in the treatment of scalp keratinocyte and skin wound healing upon activation by ligands [16, 17]. In our present investigation, we induced Keratinocyte cell line HaCaT with inflammatory agent lipopolysaccharide (LPS) and used PREO to check its anti-inflammatory efficacy. We characterized chemical composition of PREO and performed molecular docking with two prominent compounds as ligands for OR2AT4. Results indicate that PREO can decrease LPS-induced cell inflammation injury by suppressing pro-inflammatory cytokines. We also investigated whether the anti-inflammatory effect of PREO is associated with the inhibition of NF-κB pathway and oxidative stress. Our molecular docking results revealed the potential ligand activities of PREO components.

2. Materials And Methods

Chemical reagents

The PREO was donated by Jinan Wanfeng Rose Products Co. Ltd. from Pingyin, Shandong Province, China. Sodium pyruvate was purchased from Solarbio Life Sciences (Beijing, China). Dulbecco's Modified Eagle *Medium* (DMEM) and fetal bovine serum (FBS) were purchased from GIBCO BRL (Grand Island, NY, USA). The LPS (Eschenchia coli O127:B8) and the 20, 70-dichlorofluorescein-diacetate ($DCFH_2$-DA) were bought from Sigma-Aldrich (St. Louis, MO, United States). MTT assay kit, Bicinchoninic (BCA) protein assay kit, total nitric oxide (NO) assay kit, superoxide dismutase (SOD) assay kit, and malondialdehyde (MDA) assay kit were obtained from Beyotime Institute of Biotechnology, Ltd (Shanghai, China). Rabbit monoclonal antibodies against IκB-α, p-IκB-α, p65, p-p65, iNOS and Mouse monoclonal antibody against β-actin were purchased from Cell signaling technology, Danvers, United States (CST). The polymerase chain reaction (PCR) primers of β-actin, TNF-α, IL-1β, IL-6, IL-8 were acquired from BGI (Beijing Genomics Institute), China. RNA extraction kit was purchased from Transgen biotech Co Ltd (Beijing, China). High-sig ECL Western Blotting Substrate was obtained from Tanon™ (Tanon, Shanghai, China). All other chemicals used in this study were of analytical grade and purchased from Beijing Chemical Works

(Beijing, China) The PREO was dissolved in the serum-containing medium to achieve the final desired concentration.

Gas Chromatography analysis

The PREO used in this study was analyzed by gas chromatography-coupled to mass spectrometer (GC/MS). 10 µl of PREO and 1 µl of 2 - nonyl ketone was dissolved with 989 of methylene chloride, mixed well and filtered with micro syringe. Agilent GC-Mass spectrometer was used for analysis. The capillary column temperature was programmed at 50°C for 1 min, and then 10°C/min to 250°C, and finally kept at 250°C for 5 min. The injection port temperature was 260°C, while the detector temperature was 250°C. The carrier gas was helium with a flow rate of 1 mL/min. The injection volume was 1µL. Percentages of the constituents were calculated by electronic integration. Retention indices were calculated for separate relative to NIST Mass Spectral Library. The MS conditions were as follows: ionization voltage, 70eV; ion source temperature, 150°C; and electron ionization mass spectra were acquired over them mass range 50-550m/z. These specifications were like the methods used in similar research intended to determine the composition of essential oils.

Cell culture

HaCaT cells were collected from Stem Cell Bank, Institute of Zoology (China Academy of Sciences, Beijing). The cell was maintained in Dulbecco's Modified Eagle Medium (DMEM) supplemented with 10% FBS, 1% glutamax and 1% sodium pyruvate at 37°C in 5% CO_2 atmosphere. HaCaT cells were maintained in T-75 cm2 flasks (Corning Glass Works, Corning, NY). The medium was refreshed every second day.

Construction of inflammation model and cytotoxicity assay:

Cells were seeded in 96 well plates at the rate of 2×10^4 cells/well. It was cultured up to 72 hours to determine the cell growth curve. Several concentrations of LPS were used to construct an inflammation model by inducing oxidative stress in HaCaT cells. Cells were incubated with or without the addition of 2.5 µg mL^{-1}, 2 µg mL^{-1}, 1.5 µg mL^{-1}, or 1 µg mL^{-1} LPS for up to 20 h. The expressions of pro-inflammatory cytokines IL-8, IL-1β and IκB-α for 6h ,18h and 20h were determined by RT-PCR. To determine its cytotoxicity, HaCaT cells were incubated with various concentration of PREO (0.001%-1% v/v) for 20 h.

Cell viability assay

The cytotoxicity of PREO and LPS against HaCaT cells were evaluated using MTT assay. Cells were seeded in 96-well plates at 2×10^4 cells/well and cultured. After 24 h incubation period, cells were exposed to 2.5 µg/mL LPS for 20 h. Then various doses of 0.001- 0.1% (v/v) PREO were added for an additional 6–18 h. The MTT assay was performed to evaluate the cells capability.

$$\%\text{Cell viability} = \frac{\text{Absorbance of sample}}{\text{Absorbance of control}} \times 100$$

Nitric Oxide (NO) Quantification and Measurement of ROS Production

HaCaT cells were seeded at 2×10^4 cells/well in 96-well plates and incubated at 37°C for 24 h. 2.5 µg/mL LPS was added and incubated for another 20 hours. After treating with various doses of PREO for an additional 12, and 18h, cells were subjected for NO level evaluation. Nitrite was measured using Griess reagents to give an estimation of NO production. Briefly, 100µL of the cell supernatant were reacted with 100µL of Griess reagents and incubated at room temperature for 10min. Absorbance was determined at 540 µm using a spectrophotometer.

For ROS measurement, the HaCaT cells (2×10^4 cells/well in 96-well plate) were exposed to the previous series of treatment with LPS and PREO. Then following the collection, they were washed with PBS and incubated with 10µM DCFH2-DA (dissolved in PBS). After incubation, at 37℃ for 30 min, DCFH2-DA was removed and HaCaT cells were washed in PBS again. Intracellular ROS, as indicated by DCF fluorescence, was observed with a fluorescence microscope. The fluorescence intensity was quantified using a multi-detection reader at the excitation 480 nm and emission 520 nm.

Determination of MDA and SOD level in LPS induced HaCat cells

LPS induced HaCaT cells (1×10^4 per/well in a petri dish), treated with different doses of PREO, were washed twice with cold PBS, and harvested by a cell scraper. Then cell lysis fluid was added to lyse cells and supernatant from centrifugation of cells (10000g at 4℃ for 5min) was collected. The content of MDA and SOD activity were determined using the commercial kits and by following the manufacturer's instructions.

Quantitative real-time polymerase chain reaction (qRT-PCR)

Following the manufacturer's instructions, the total RNA from the HaCaT cells (5×10^6 cells/well in petri dish treated with LPS and PREO) was isolated using a Trizol reagent. The concentration and integrity of the RNA were measured at a 260/280 nm ratio. 0.5 µg of RNA was reverse-transcribed using the Prime Script RT reagent kit for the cDNA synthesis. The PCR primers were designed using NCBI, and the primer sequences have been presented in Table 2. As invariant housekeeping gene internal control, the β-actin gene was used. Briefly, the reaction series was as follows: 50℃ for 2 min, 95℃ for 30 s for one cycle; then 95℃ for 5 s, 59℃ for 15 s, and 72℃ for 45 s for 40 cycles. The relative gene expression was quantified by the comparative $2^{-\Delta\Delta CT}$ method [18]. All the reactions were conducted in triplicate.

Western Blotting Analysis

After treatment, the HaCaT cells (5×10^6 cells/well in a petri dish) were collected and the total protein was extracted using cell lysis buffer for Western blot containing protease inhibitors or phosphatase inhibitors. Then, the solution was kept in ice for 30 min and later centrifuged at 3000 rpm for 15 min at 4°C. The supernatants were separated and protein concentrations were quantified by using BCA protein assay following the microplate procedure. 30 µg proteins from each sample were separated by sodium dodecyl

sulfate-polyacrylamide gel electrophoresis (SDS-PAGE) and then transferred to (PVC) polyvinylidene difluoride membrane (Merck KGaA, Darmstadt, Germany). The membrane was blocked at 4°C with 5% non-fat milk in tris-buffer saline (TBST). The membrane was then incubated with primary antibodies, and then washed with TBST thrice. After that, the membrane incubated with secondary antibodies for 2 hours at room temperature. Finally, Tanon™ High-sig ECL Western Blotting Substrate (Tanon, Shanghai, China) was applied to the membrane to visualize the band density as per manufactures instruction. Finally, using ImageJ image processing software (ImageJ, National Institutes of Health, USA), bands were quantified as per their density and evaluated.

Molecular Docking

The sequence of OR2AT4 was retrieved from Uniprotkb database (https://www.uniprot.org/). The accession number was A6NND4. The sequence was BLAST to find out similar hit. ProtParam (https://web.expasy.org/protparam/) was used to analyze the secondary structure. TMHMM 2.0 (https://services.healthtech.dtu.dk/service.php?TMHMM-2.0) and PSIPRED (http://bioinf.cs.ucl.ac.uk/psipred) were used to predict and analyze OR2AT4 structure including transmembrane regions, amino acid polarity, potential domain and secondary structure. Based on the BLAST result of PSI-BLAST (https://blast.ncbi.nlm.nih.gov), a best template was selected according to the percentage of sequence coverage, E-value ,species and percentage of sequence similarity. PDB (protein databank; https://www.rcsb.org) was used to download the best template (PDB id :7mbx; resolution 1.9A^0). This structure was used to predict 3D homology model of OR2AT4 by Swiss-Modeller [19]and Modeller 10.2 [20]. I-tasser [21] online service was also used to predict the 3D structure. The Ab-initio 3D structure of OR2AT4 was designed with trRosetta [22]. Model evaluation was done by SAVES v6.0 server depending on ERRAT, VERIFY3D and PROCHECK. The top two component of PREO from GC-MS result was selected based on their relative area percentage. These two compounds were downloaded as sdf format from Pubchem and were prepared as ligands for docking (https://pubchem.ncbi.nlm.nih.gov). Before docking analysis, both ligands and receptor OR2AT4 were optimized by Autodock Tool software (ADT4). Ligand binding sites and pockets were predicted by CastP [23]. Then AutoDoc Vina was used to perform molecular docking [24].

Statistical Analysis

All values were expressed as mean ± SD of three parallel measurements and the analysis was carried out in triplicate. Statistical analysis was carried out by a one-way analysis of variance (ANOVA) test using a statistical package program (SPSS 13.0) and the significance of the difference between means was determined by Duncan's multiple range test at ($p < 0.05$) a significant level [25].

3. Results

GC-MS analysis of PREO

From the GC-MS analysis shown in Table 1, 57 compounds were determined. Mostly are terpenoids and monoterpenoids. The most significant two compounds are Citronellol, and Geraniol. Citronellol is a natural monoterpenoid, geraniol is a both monoterpenoid and alcohol.

The GC-MS chromatogram tracing and quantitative analysis of active constituents is shown as Table 1.

Effects of LPS and PREO individually on HaCaT cells

As shown in Fig. 1(B), LPS up to 2.5 μg/ml do not have any cytotoxicity. However, the expressions of pro-inflammatory cytokines in different incubation period determined the oxidative stress level. After 20hrs of incubation (Fig. 1A), IL-8, IL-1β and IκB-α expressions were almost doubled compared to control (no-LPS). For 6h,12h and 18h, expressions were not very significant to be considered as inflammation model. However, from our result, LPS can induce oxidative stress in HaCaT cells in a dose-time dependent manner. In case of PREO induced MTT assay, cells show decrease in viability with the increase of concentration after 24 h. According to Fig. 1C, the highest concentration was 1%, which is visibly toxic to cells. So, LPS 2.5 μg/ml and 0.001%-0.1% PREO had been used for further explorations as they promote cell growth without affecting cell viability.

Effects of PREO on LPS-induced HaCaT cell viability

After treated with 2.5 ug/ml of LPS for 20 h, the cells were treated with 0.001-0.1% (v/v) PREO for 6–18 h to determine the protective effects of PREO on LPS induced cell viability loss. LPS showed a slight decrease in cell viability after 6h of inductions which was regained after 18h probably because of cell adaptation. The results showed that LPS and PREO had promoted cell growth, and the cell survival rate was 90% and above (Fig. 1D).

Effects of PREO on NO and ROS production in LPS induced HaCaT cells

NO and ROS are one of the main criteria for producing oxidative stress. PREO was evaluated with Griess reagent method to determine its effect on reduction of NO level in LPS-induced HaCaT cells. As shown in Fig. 2A, the levels of NO markedly increased in response to 20h induction of LPS. Treatment with 0.001%, 0.01% and 0.1% PREO showed no effects on the NO level after 6 h, but after 12h of induction, PREO reduced the NO level notably and after 18h 0.001% and 0.1% PREO decreased it further more. To determine the cytoprotective effects of PREO in LPS-stimulated HaCaT cells, ROS levels were measured via fluorescent probe DCFH-DA. LPS increased the ROS level in a high range. Conversely, treatment with 001%, 0.01% and 0.1% PREO for 12h significantly reduced ROS levels but both 6h and 18h incubation showed slight raise compared to control (Fig. 2B). These results indicate that PREO can possibly restore the endogenous antioxidant defense mechanisms impaired by LPS. The above findings indicated that the effects of PREO on ROS level were related to the concentration of PREO and induction time.

Effects of PREO on activity of SOD and production of MDA

SOD and MDA are the key markers of oxidative stress. Respective kits measured the levels of SOD activity and MDA content. As shown in Fig. 3 (A, B), LPS induction reduced the activity of SOD but it was remarkably increased at 0.1% of PREO treatment for 6h and showed decrease after 18h (compared to 6 h) in LPS-induced HaCaT cells. The MDA levels markedly increased in response to 20 h of LPS stimulation, whereas treatment with PREO significantly inhibited it in time and dose dependent manner. PREO treated at 0.001% concentration for 6h did not reduce the production of MDA, it is possibly because the treatment time was too short and the concentration was too low. These results showed that PREO could alleviate the oxidative stress to adjust the effect of inflammation.

Effects of PREO on inflammatory cytokines production in mRNA level

One of the most obvious initial changes due to inflammation is the increase of inflammatory cytokines expression levels. IL-1β, IL-6, IL-8 and TNF-α are the most common cytokines over expressed due to inflammation. As shown in Fig. 4, the mRNA production of IL-1β, IL-6, IL-8 and TNF-α in LPS-induced HaCaT cells markedly increased in response to the LPS ($p < 0.05$) compared to control group both after 6h and 18h of induction. Treatment with 0.001%, 0.01% and 0.1% PREO significantly reduced LPS-induced mRNA level activation of IL-1β, IL-6, IL-8 and TNF-α in a time and dose-dependent manner compared to only LPS exposed HaCaT cells (Fig. 4A-D). After 6h of treatment, PREO significantly decreased the transcription level of the cytokines, while after 12 h and 18h of inductions caused more reductions with time. 0.001% PREO showed same results as control after 18h of incubation following further decrease with 0.01% and 0.1% PREO. Together, the above results indicated that PREO is a potent inhibitor of LPS-induced inflammatory cytokines expressions.

Effects of PREO on the NF-κB production and phosphorylation of related proteins

The production of inflammatory mediators is strongly affected by NF-κB pathways in the HaCaT cells. p65 and IκB-α are the major component of NF-κB activated by LPS in the HaCaT cells. As shown in Fig. 5 (A-D), LPS remarkably increased that expression of p65 and IκB-α and promoted their phosphorylation. Furthermore, concentration of 0.01% PREO can significantly reduce the expression of p65 and IκB-α and inhibit the phosphorylation of p65 and IκB-α in HaCaT cells after 18h of incubation (Fig. 5B, D). These experimental findings hint that PREO can mediate the inflammation in the HaCaT cells induced by LPS through NF-κB pathways.

Effects of PREO on TLR4 pathway in LPS-induced HaCaT cells

As LPS is a well-known ligand of TLR4, we evaluated the level of mRNA expression involved in this pathway. MyD88, TBK1, Cas-8, TRAK-4, TAK1, IKKβ, IKKΣ, p38 and TRIF mRNA expression levels were measured using RT-PCR analysis. We chose to treat the cell with 0.01% PREO for 18 h following 20 h of LPS pre-induction. We also exposed the cell to only 0.01% PREO to check its individual effects (Fig. 6)

LPS significantly raise the expression level for all mRNA compared to control. This refers to LPS boosting their expression. However, 18 h of exposure with 0.01% of PREO on LPS induced cells relatively lowers the

inflammation level. When cells were treated with 0.01% PREO without LPS, MKK5, TAK1, IKKβ, IKKΣ, p38 and TRIF mRNA expression levels were increased compared to normal cell. MyD88, TBK1, MKK5 and TRAK-4 expression had slight changes while Cas9 showed decreased expression in LPS free PREO induced cells.

Binding affinity of ligands with OR2AT4

The physiochemical properties of OR2AT4 were represented in Table 3. The 7TM region was represented in Fig. 7B. Depending on the results from Saves v.6 (Table 4). the model from I-Tasser was selected for modeling. The evaluation results were shown in Fig. 7B, C. The Ramachandran plot showed 82.8% of amino acids in favored region while ERRAT value was 94.15 and verify3D value was 57.19%. This result revealed that the predicted model had very little local errors, compatible with amino acid sequence and conformation of the chain was acceptable for docking. The binding sites for OR2AT4 were 1, 6, 11, 16, 18, 19, 21, 23, 24, 29, 36, 78, 82, 83, 85, 86, 89, 90, 93, 94, 105, 106, 109, 110, 112, 113, 114, 164, 165, 167, 168, 180, 182, 183, 184, 185, 186, 188, 189, 190, 200, 203, 204, 207, 208, 211, 212, 256, 257, 260, 261, 263, 264, 267, 274, 277, 278, 280, 281, 284, 285, 288 residues. Geraniol (compound ID = 637566) and Citronellol (compound ID = 8842) were used as ligands. The binding affinity for the best predicted model geraniol was − 5.6 kcal and for citronellol its − 5.5 kcal. The binding pocket of Geraniol was Pro63, Phe67, Val122, Tyr125, Met141, Leu149, Asp126, Tyr 137, Asn146 and the binding pocket of citronellol was Val122, Tyr125, Val129, Met141, Asn146, Leu149, Pro63, Phe67, Asp126, Tyr137, Leu 140. All the docking results were presented in Table 5. Protein structure (ribbon) and ligands was presented in Fig. 7A, F-G. The interactions were presented in 2D format for individual proteins in Fig. 7H, I. The docked model with protein ligand interaction was presented in Fig. 7.

4. Discussion

It has been reported that geraniol and citronellol are excellent anti-inflammatory monomers. Most of the EOs are full of versatile small compounds so basically the biofunctions of the EOs may possibly be determined by its' main components [5, 26, 27]. From our PREO GC-MS analysis, it is evident that citronellol and geraniol combinedly 63.54% of total oil which is very high amount compared to other rose oil. The GC-MS for oil of *Rosa damascena* revealed that main components are citronellol (20.8 %) and noadecane (8.5 %) [28]. Howver, there is a few reports on the effects of REO against skin inflammation.

One of the mechanisms by which PREO exerts anti-inflammatory effects is to inhibit the expression of pro-inflammatory factors (IL-1β, IL-6, IL-8 and TNF-α). Upon exposure of LPS, the expressions of inflammatory cytokines raised almost doubled, but PREO can significantly suppress them. The mRNA expression of three inflammatory cytokines in 0.1% PREO for 18h group has the best effects (Fig. 4). It is very similar to control group. A study on LPS induced human THP-1 cells exposed to three different Asian herbs essential oil (*C. martinii*, *T. vulgaris*, and *P. aeruginosa*) showed limitation effects on the secretion levels of TNF-α and IL-1β in LPS [29].

Oxidative stress is involved in the occurrence and development of many diseases, and it is an important pathogenic factor of inflammatory response. Therefore, reduce the oxidative level is an important direction to inhibit inflammation. NO is the free radical product of the oxidative deamination of L-arginine which made it a prominent oxidative marker. Many studies suggested that, different essential oil could reduce the tissue injury by decreasing NO and ROS level [30–33]. In evaluation of the effects of PREO on NO production with griess reagent method, our results showed PREO can suppress NO production levels in a significant way to alleviate oxidative stress in cells ($p < 0.05$). Our previous study found that PREO could inhibited the expression of iNOS in LPS-induced RAW264.7 cells, which is also one of its anti-inflammatory mechanisms. During inflammation, iNOS is up-regulated and produces large amounts of NO, which plays an important role as a signaling molecule in various physiological processes. Upregulation of iNOS is one of the indicators for activation of NF-κB signaling [14, 34]. ROS induces inflammation by stimulating MAPKs, Akt, NF-κB pathway [35, 36]. The model used in the present study increases the generation of free radicals and other ROS in the HaCaT cells. Any imbalance between the production of these molecules and their safe disposal may culminate in oxidative stress. In our study, PREO decreased ROS production in the LPS-induced HaCaT cells. It showed that PREO could induce oxidative stress to a certain extent (Fig. 2).

SOD and MDA are considered common indicators of oxidative stress and play a key role to maintain cell redox homeostasis [37, 38]. SOD can catalyze the conversion of O_2^- into H_2O_2 and O_2. H_2O_2 is the one of ROS, which can lead to the continuous occurrence of oxidative stress if it is excessive [39, 40]. The result from our experiment showed that LPS could reduce the activities of SOD, while PREO can be beneficial in decreasing the activities of the enzyme in the HaCaT cells induced by LPS. MDA is the final product of polyunsaturated fatty acids and lipids, and is considered an important factor for studying oxidative stress. The degree of oxidative stress gets low with the reduction of MDA level (Ito et al., 2019). In our study, PREO (after 18h) can lower the MDA level of HaCaT cells (Fig. 3A). According to other researches, ginger EO and *Piper nigrum Linn* EO can raise SOD activity in formalin induced BALb/c mice [41, 42].

We examined the effect of PREO on the activation of NF-κB in the HaCaT. The data are consistent with ROS production that PREO significantly reduced phosphorylation level of P65 and Iκb-α. Increase in phosphorylation of IκBα connected with NF-κB and p65 was done by these two adaptor proteins [43, 44]. PREO, after 18h of incubation can inhibit the translocation of NF-κB through reducing the phosphorylation of NF-κB p65 and IκB-α (Fig. 5). The binding of NF-κB p50 and NF-κB p65 induce translocation and promote of TNF-α, IL-6 and other inflammatory cytokines. The phosphorylated Iκbα is degraded by ubiquitin-proteasome system to free NF-κB that translocate from cytoplasm to nucleus and induces many target genes expressions [43, 45, 46]. As PREO minimizes the phosphorylation, it consequently downregulates the aftermath.

TLR4 binds with LPS and activates myeloid differentiation primary response 88 (MyD88) and TIR-domain-containing adapter-inducing interferon-β. Genes that involved in TLR4-NF-κB signaling pathway are MyD88, TBK1, Cas-9, MKK5, TRAK-4, TAK1, IKKβ, IKKΣ, p38 and TRIF [47]. In our study, we exposed HaCaT cells with or without LPS to 0.1% PREO to find out its involvement in downregulating TLR4

pathway. MKK5, TAK1, IKKβ, IKKΣ, p38 and TRIF mRNA expression levels were escalated compared to control in PREO treated cells (No LPS). MyD88, TBK1, MKK5 and TRAK-4 expression had little wavers while Cas9 showed reduced expression in PREO induced cells without LPS. On the other hand, LPS increased the mRNA expression level for all mRNA. 0.1% PREO significantly lowered the level in LPS induced cells compared to LPS group (Fig. 6).

While docking with human OR2AT4, citronellol and geraniol showed fewer binding affinities and lower RMSD (Fig. 7). From the analysis, overall geraniol had the most effective results. Hence if we consider the percentages, it is more likely that citronellol is the key inhibitor as its affinities were lower like geraniol (Table 5). OR2AT4 is a prominent skin EOR [48]. OR2AT4 expression is very high in basal keratinocytes. Binding with sandalore could speed up proliferation and migration of keratinocyte resulting in wound healing [16]. The growth of hair follicles can also increase by stimulated OR2AT4 [17]. Hence, OR2AT4 possibly can be involved in inflammation process too. In addition, as it is an olfactory receptor, the binding with aromatic compounds from PREO is predicted to happen. From our analysis result, Geraniol and citronellol are promising ligands for OR2AT4. The binding affinity for best docked were − 5.6 kcal for geraniol which means the molecule was interacting with van der wales bond and need energy of 5.1 kcal. For citronellol, the energy needed was − 5.5 kcal (Table 5). All these outcomes made geraniol and citronellol as strong candidates for OR2AT4 ligands which need thorough investigation in future.

5. Conclusion

Skin inflammation can be life threatening consequently as skin is the primary defense interface of our body against outside environment. However, PREO is a potential anti-inflammatory agent for the remedy of skin related inflammations.

The GC-MS analysis showed that the most prominent components are citronellol, and geraniol. Our investigation showed that PREO has protective effects on LPS induced HaCaT cells. After conducting a series of experiments that included RT-PCR and western blot, NF-κB signaling is found to be possibly downregulated by PREO through lowering the expression of prominent pro-inflammatory genes and obstructs phosphorylation of NF-κB p65 and IκB-α. In addition, PREO limits down NO and ROS productions revealing its soothing effects on oxidative stress. Docking results put a new light on the possibility of screening new ligands for OR2AT4. All these results manifest the noteworthy potential of PREO as an anti-inflammatory agent for skin and its principal two components as potential ligands for OR2AT4. Further investigation in future can make opportunities to consider PREO as a promising treatment option.

6. Abbrebiation

TCM, Traditional Chinese medicines; **PREO,** Pingyin rose essential oil; **LPS,** lipopolysaccharides; **MDA**, malondialdehyde; **SOD**, Superoxide dismutase; **ROS,** reactive oxygen species; **NO**, nitric oxide; **TLR4**, toll-like receptor 4; **NF-κb,** Nuclear factor kappa B; **TNF-α,** Tumor necrosis factor alpha; **IL**, Interleukin; **DMEM,**

Dulbecco's Modified Eagle *Medium;* ***FBS,*** fetal bovine serum; **$DCFH_2$-DA,** dichlorofluorescein-diacetate; **BCA,** Bicinchoninic; **GC-MS,** gas chromatography-coupled to mass spectrometer; **SDS-PAGE,** sodium dodecyl sulfate-polyacrylamide gel electrophoresis; **iNOS,** inducible nitric oxide synthetase; **PVC,** polyvinylidene difluoride; **TBST,** tris-buffer saline; **PDB,** Protein data bank; **ANOVA,** one-way analysis of variance.

Declarations

7.1 Conflict of interest

There is no conflict to declare.

7.2 Data Availability

The data used to support the findings of this study are available as supplementary data

7.3 Acknowledgement/Funding

This research was supported Beijing municipal education commission general project (KM202010011010) and Beijing Natural Science Foundation (Grant No. 6212002).

7.4 Author's contribution

Song Jingyi:- Methodology, Data Curation , Formal Analysis; Raka Rifat Nowshin:- Paper Writing (Original draft), editing and reviewing; Yuan Yue and Park Suyeon:- Visualization and analysis; Wang Juan:- Methodology; Liu Fei:- Data Curation; Dr. Wu Hua :- Conceptualization , Project administration ,Fund acquisition, Paper writing, Editing, reviewing; Dr. Xiao Junsong:-Fund acquisition, Conceptualization; Huang Mingquan and Yang Suzhen:- reviewing

7.5 Ethics approval and consent to participate

Not applicable

7.6 Consent for publication

Not applicable

References

1. He Y, Kim BG, Kim HE, Sun Q, Shi S, Ma G, et al. The protective role of feruloylserotonin in LPS-induced HaCaT cells. Molecules. 2019;24.
2. Qu R, Chen X, Hu J, Fu Y, Peng J, Li Y, et al. Ghrelin protects against contact dermatitis and psoriasiform skin inflammation by antagonizing TNF-α/NF-κB signaling pathways. Scientific Reports. 2019;9.

3. Pasparakis M, Haase I, Nestle FO. Mechanisms regulating skin immunity and inflammation. Nature Reviews Immunology. 2014;14:289–301.
4. Mahboubi M, Feizabadi MM, Khamechian T, Kazempour N, Zadeh MR, Sasani F, et al. The Effect of Oliveria Decumbens and Pelargonium Graveolens on Healing of Infected Skin Wounds in Mice.
5. Wang J, Su B, Zhu H, Chen C, Zhao G. Protective effect of geraniol inhibits inflammatory response,oxidative stress and apoptosis in traumatic injury of the spinal cord through modulation of NF-κb and p38 MAPK. Experimental and Therapeutic Medicine. 2016;12:3607–13.
6. Bedi MK, Shenefelt PD. Herbal Therapy in Dermatology.
7. Hon KL, Chan BC, Leung PC. Chinese herbal medicine research in eczema treatment. Chinese Medicine. 2011;6.
8. Pan MH, Chiou YS, Tsai ML, Ho CT. Anti-inflammatory activity of traditional chinese medicinal herbs. Journal of Traditional and Complementary Medicine. 2011;1:8–24.
9. Shenefelt PD. Herbal Medicine: Biomolecular and Clinical Aspects.
10. Ng TB, He JS, Niu SM, Pi ZF, Shao W, Liu F, et al. A gallic acid derivative and polysaccharides with antioxidative activity from rose (Rosa rugosa) flowers. Journal of Pharmacy and Pharmacology. 2010;56:537–45.
11. Liu L, Tang D, Zhao H, Xin X, Aisa HA. Hypoglycemic effect of the polyphenols rich extract from Rose rugosa Thunb on high fat diet and STZ induced diabetic rats. Journal of Ethnopharmacology. 2017;200:174–81.
12. Lu J, Wang C. Medicinal components and pharmacological effects of rosa rugosa. Records of Natural Products. 2018;12:535–43.
13. Tung YT, Chua MT, Wang SY, Chang ST. Anti-inflammation activities of essential oil and its constituents from indigenous cinnamon (Cinnamomum osmophloeum) twigs. Bioresource Technology. 2008;99:3908–13.
14. Wu Y, Antony S, Meitzler JL, Doroshow JH. Molecular mechanisms underlying chronic inflammation-associated cancers. Cancer Letters. 2014;345:164–73.
15. Borges RS, Ortiz BLS, Pereira ACM, Keita H, Carvalho JCT. Rosmarinus officinalis essential oil: A review of its phytochemistry, anti-inflammatory activity, and mechanisms of action involved. Journal of Ethnopharmacology. 2019;229:29–45.
16. Busse D, Kudella P, Grüning NM, Gisselmann G, Ständer S, Luger T, et al. A synthetic sandalwood odorant induces wound-healing processes in human keratinocytes via the olfactory receptor OR2AT4. Journal of Investigative Dermatology. 2014;134:2823–32.
17. Chéret J, Bertolini M, Ponce L, Lehmann J, Tsai T, Alam M, et al. Olfactory receptor OR2AT4 regulates human hair growth. Nature Communications. 2018;9.
18. Livak KJ, Schmittgen TD. Analysis of relative gene expression data using real-time quantitative PCR and the 2-ΔΔCT method. Methods. 2001;25:402–8.

19. Waterhouse A, Bertoni M, Bienert S, Studer G, Tauriello G, Gumienny R, et al. SWISS-MODEL: Homology modelling of protein structures and complexes. Nucleic Acids Research. 2018;46:W296–303.
20. Webb B, Sali A. Comparative protein structure modeling using MODELLER. Current Protocols in Bioinformatics. 2016;2016:5.6.1–5.6.37.
21. Contributions A. performed research and created and tested the I-TASSER Suite package. Z Nat Methods. 2015;12:7–8.
22. Du Z, Su H, Wang W, Ye L, Wei H, Peng Z, et al. The trRosetta server for fast and accurate protein structure prediction. Nature Protocols. 2021;16:5634–51.
23. Tian W, Chen C, Lei X, Zhao J, Liang J. CASTp 3.0: Computed atlas of surface topography of proteins. Nucleic Acids Research. 2018;46:W363–7.
24. Trott O, Olson AJ. AutoDock Vina: Improving the speed and accuracy of docking with a new scoring function, efficient optimization, and multithreading. Journal of Computational Chemistry. 2009;:NA-NA.
25. IBM Corp. IBM SPSS Statistics for Windows [Internet]. Armonk, NY: IBM Corp; 2017.
26. Brito RG, Guimarães AG, Quintans JSS, Santos MRV, de Sousa DP, Badaue-Passos D, et al. Citronellol, a monoterpene alcohol, reduces nociceptive and inflammatory activities in rodents. Journal of Natural Medicines. 2012;66:637–44.
27. Gogoi R, Loying R, Sarma N, Begum T, Pandey SK, Lal M. Comparative Analysis of In-Vitro Biological Activities of Methyl Eugenol Rich Cymbopogon khasianus Hack., Leaf Essential Oil with Pure Methyl Eugenol Compound. Current Pharmaceutical Biotechnology. 2020;21:927–38.
28. Ahmad A, Sahoo D, Ahmad J, Tandon S. GC-MS Composition of Rose Oil (Rosa damascena) of Different Agro Climatic Regions of North India †. 2009.
29. Tsai ML, Lin CC, Lin WC, Yang CH. Antimicrobial, antioxidant, and anti-inflammatory activities of essential oils from five selected herbs. Bioscience, Biotechnology and Biochemistry. 2011;75:1977–83.
30. Siramon P, Ohtani Y. Antioxidative and antiradical activities of Eucalyptus camaldulensis leaf oils from Thailand. Journal of Wood Science. 2007;53:498–504.
31. Salem MZM, Elansary HO, Ali HM, El-Settawy AA, Elshikh MS, Abdel-Salam EM, et al. Bioactivity of essential oils extracted from Cupressus macrocarpa branchlets and Corymbia citriodora leaves grown in Egypt. BMC Complementary and Alternative Medicine. 2018;18.
32. Okuda-Hanafusa C, Uchio R, Fuwa A, Kawasaki K, Muroyama K, Yamamoto Y, et al. Turmeronol A and turmeronol B from: Curcuma longa prevent inflammatory mediator production by lipopolysaccharide-stimulated RAW264.7 macrophages, partially via reduced NF-κB signaling. Food and Function. 2019;10:5779–88.
33. Ho CL, Li LH, Weng YC, Hua KF, Ju TC. Eucalyptus essential oils inhibit the lipopolysaccharide-induced inflammatory response in RAW264.7 macrophages through reducing MAPK and NF-κB pathways. BMC complementary medicine and therapies. 2020;20:200.

34. Vendramini-Costa DB, Carvalho JE. Molecular Link Mechanisms between Inflammation and Cancer. 2012.
35. Son Y, Cheong Y-K, Kim N-H, Chung H-T, Kang DG, Pae H-O. Mitogen-Activated Protein Kinases and Reactive Oxygen Species: How Can ROS Activate MAPK Pathways? Journal of Signal Transduction. 2011;2011:1–6.
36. CIRCRESAHA.117.311401.
37. Valko M, Leibfritz D, Moncol J, Cronin MTD, Mazur M, Telser J. Free radicals and antioxidants in normal physiological functions and human disease. The International Journal of Biochemistry & Cell Biology. 2007;39:44–84.
38. Ho E, Karimi Galougahi K, Liu CC, Bhindi R, Figtree GA. Biological markers of oxidative stress: Applications to cardiovascular research and practice. Redox Biology. 2013;1:483–91.
39. Dröge W. Free radicals in the physiological control of cell function. Physiological Reviews. 2002;82:47–95.
40. Yang HY, Lee TH. Antioxidant enzymes as redox-based biomarkers: A brief review. BMB Reports. 2015;48:200–8.
41. Kuttan R, Jeena K, Liju VB. ANTIOXIDANT, ANTI-INFLAMMATORY AND ANTINOCICEPTIVE ACTIVITIES OF ESSENTIAL OIL FROM GINGER. 2013.
42. Jeena K, Liju VB, Umadevi NP, Kuttan R. Antioxidant, Anti-inflammatory and Antinociceptive Properties of Black Pepper Essential Oil (Piper nigrum Linn). Journal of Essential Oil-Bearing Plants. 2014;17:1–12.
43. Verstrepen L, Bekaert T, Chau TL, Tavernier J, Chariot A, Beyaert R. TLR-4, IL-1R and TNF-R signaling to NF-κB: Variations on a common theme. Cellular and Molecular Life Sciences. 2008;65:2964–78.
44. Christian F, Smith EL, Carmody RJ. The regulation of NF-κB Subunits by Phosphorylation. Cells. 2016;5.
45. Werlen G, Jacinto E, Xia Y, Karin M. Calcineurin preferentially synergizes with PKC-θ to activate JNK and IL-2 promoter in T lymphocytes. 1998.
46. Chen J, Chen ZJ. Regulation of NF-κB by ubiquitination. Current Opinion in Immunology. 2013;25:4–12.
47. Pålsson-McDermott EM, O'Neill LAJ. Signal transduction by the lipopolysaccharide receptor, Toll-like receptor-4. Immunology. 2004;113:153–62.
48. Raka RN, Wu H, Xiao J, Hossen I, Cao Y, Huang M, et al. Human ectopic olfactory receptors, and their food originated ligands: a review. Critical Reviews in Food Science and Nutrition. 2021.

Tables

Table 1
Main compounds detected in PREO through GC-MS analysis

No.	RI	Compounds	Relative peak area (%)
1	1028	α-Pinene	0.73
2	1112	β-Pinene	0.10
3	1124	2,4(10)-Thujadiene	0.02
4	1161	β-Myrcene	0.06
5	1184	Heptanal	0.12
6	1199	L-Limonene	0.13
7	1213	Eucalyptol	0.02
8	1231	2-Pentylfuran	0.03
9	1250	trans-β-Ocimene	0.07
10	1250	β-Ocimene	0.07
11	1275	o-Cymene	0.04
12	1283	Terpinolene	0.05
13	1282	trans-2-(2-Pentenyl) furan	0.02
14	1320	2-Heptanol	0.05
15	1338	5-Hepten-2-one	0.02
16	1365	Rose oxide	0.91
17	1367	trans-Rose oxide	0.32
18	1413	Rosefuran	0.01
19	1429	Perillen	0.02
20	1435	Ethyl octanoate	0.02
21	1444	p-Cymenene	0.02
22	1450	1-Octene-3-ol	0.01
23	1465	6-Methyl-5-hepten-2-ol	0.01
24	1469	Nerol oxide	0.05
25	1495	Daucene	0.20
26	1514	Cyclohexane	0.24
27	1547	β-Linalool	1.36

No.	RI	Compounds	Relative peak area (%)
28	1579	trans-α-Bergamotene	0.28
29	1586	β-Copaene	0.21
30	1598	methyl nonyl ketone	0.26
31	1615	Citronellyl formate	0.15
32	1639	Isosativene	0.11
33	1660	Citronellol acetate	3.35
34	1661	α-Himachalene	0.58
35	1728	Naphthalene	0.30
36	1727	β-Bisabolene	0.17
37	1735	Bicyclogermacren	0.85
38	1746	α-Farnesene	2.01
39	1753	Geranyl acetate	1.00
40	**1765**	**Citronellol**	**54.37**
41	1797	cis-Geraniol	4.20
42	1809	Tridecanone	1.85
43	1813	Phenethyl acetate	0.24
44	**1847**	**Geraniol**	**9.26**
45	1903	2-Tridecanol	0.15
46	1906	Pheneylethyl alcohol	1.28
47	2013	Methyleugenol	3.99
48	2098	Tetradecanol acetate	0.56
49	2100	Heneicosane	2.26
50	2108	Pentadecanol	0.04
51	2123	Cyclododecanol	0.07
52	2165	1-Tetradecanol	0.14
53	2169	Eugenol	1.40
54	2215	α-Bisabolol	0.67
55	2500	Pentacosane	4.66

No.	RI	Compounds	Relative peak area (%)
56	2350	Farnesol	0.40
57	2599	15-Hydroxy-α-muurolene	0.45
Total			99.83%

Table 2
Primers for RT-PCR analysis of relative genes

Name	Forward	Reverse
β-actin	CCTAGA AGC ATT TGCGGTGCACGATG	TCATGAAGTGTGACGTTGACATCCGT
IL-6	AAGTGCATCATCGTTGTTCATACA	GAGGATACCACTCCCAACAGACC
IL-1β	GTGCTGCCTAATGTCCCCTTGAAT	TGCAGAGTTCCCCAACTGGTACAT
TNF-α	TACAGGCTTGTCACTCGAATT	ATGAGCACAGAAAGCATGATC
IκBα	AACCTGCAGCAGACTCCACT	ACACCAGGTCAGGATTTTGC
IL-8	CTGATTTCTGCAGCTCTGTG	GGGTGGAAAGGTTTGGAGTATG
MyD88	TGCTCGAGCTGCTTACCAAG	CATCCGGCGGCACCAATG
IRAK-4	TCATGGCTGTTTCTGGCTGT	CCCAGATACAACCCCGCAAT
IKKβ	GTGGTTGTCCTCTTTTCGGC	AAGCTCACAGCCCTTAGCC
TKB1	GAGGAGGCCGCGGGA	AGAACCTGAAGACCCCGAGA
TAK1	CTTGCAGACTGGTCCTCTGG	TGGCGCCAAATCCTGAGGTAA
IKKΣ	AGAGGTACTCCTGGTGTCGG	GAGTGTGGGAAATCCGGAGA
P38MAPK	ATCCTCAGGCATGGAACGTG	ACTCCTTTGAGCCGTTTGGA
TRIF	CTGAGTGGTCTATGGCGTCC	TTGGAAATCAGCCAGTCCCC
Caspase-8	GCTCTTCAAAGGTCGTGGTCA	CTGAGCTGGTCTGAAGGCTGG

Table 3
Physiochemical properties of OR2AT4

Parameters	Details		
Molecular weight	98553.79		
Theoretical pI	5.50		
Estimated half-life	1.9 hour (mammalian reticulocytes, in vitro) > 20 hours (yeast, in vivo)		
Total Negatively charged residues	92		
Total Positively charged residues	63		
GRAVY	-0.575		
Outside Membrane	1–31		
TM helix	TM helix 1	32–54	
	TM helix 2	66–83	
	TM helix 3	103–125	
	TM helix 4	146–168	
	TM helix 5	201–223	
	TM helix 6	243–265	
	TM helix 7	275–297	
Amino Acids (%)	Ala (A)	51	6.8%
	Arg (R)	61	8.2%
	Asn (N)	35	4.7%
	Asp (D)	21	2.8%
	Cys (C)	5	0.7%
	Gln (Q)	0	0%
	Glu (E)	71	9.5%
	Gly (G)	5	0.7%
	His (H)	30	4.0%
	Ile (I)	31	4.2%
	Leu (L)	58	7.8%
	Lys (K)	2	0.3%

Parameters	Details		
	Met (M)	42	5.6%
	Phe (F)	16	2.1%
	Pro (P)	20	2.7%
	Ser (S)	49	6.6%
	Thr (T)	96	12.9%
	Trp (W)	43	5.8%
	Tyr (Y)	4	0.5%
	Val (V)	5	0.7%
	Pyl (O)	79	10.6
	Sec (U)	10	1.3

Table 4
Evaluation results of OR2AT4 3D structures

Model	Server	ERRAT	Verify 3D(%)	PROCHECK		
				Favored region (%)	Allowed region (%)	Disallowed region (%)
Homologues Modelling	Modeller	32.13	31.56	86.6	10.3	1.4
	SWISS-MODEL	89.74	24.04	93.5	5.3	0.4
	I-Tasser	94.55	57.19	82.8	14.1	1.0
Ab -initio	trRosetta	95.17	68.75	93.5	6.5	0.0

Table 5
Molecular docking values with human proteins and ligands

Protein	Compound	Binding affinity	Interaction	
		((kcal/mol)	H/Alkyl/Covalent bonds	Van der wales bond
OR2AT4	Geraniol	-5.6	Pro63, Phe67, Val122, Tyr125, Met141, Leu149	Asp126, Tyr 137, Asn146
	Citronellol	-5.5	Val122, Tyr125, Val129, Met141, Asn146, Leu149	Pro63, Phe67, Asp126, Tyr137, Leu 140

Figures

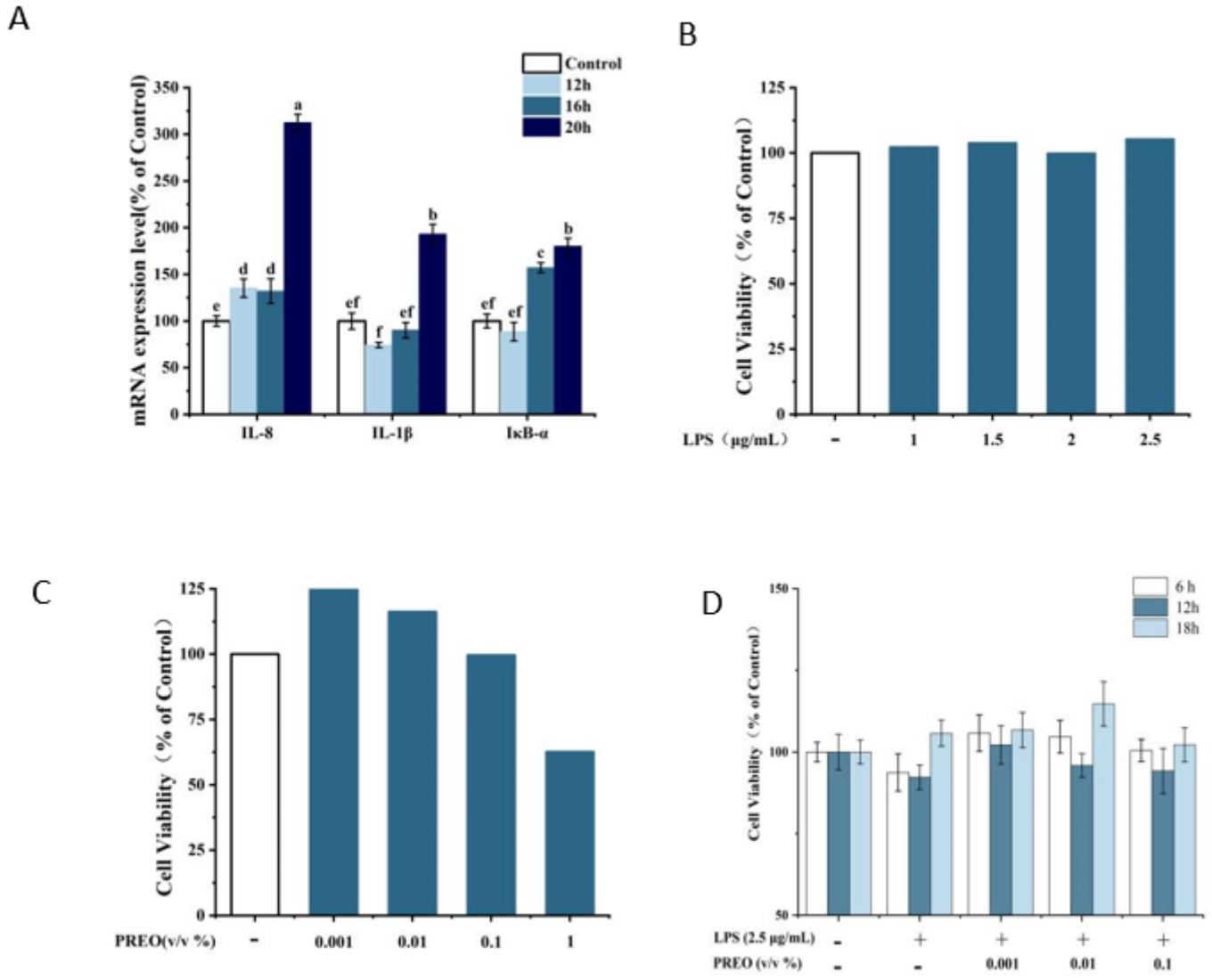

Figure 1

Construction of inflammation model in HaCaT cell with LPS. (A) The effects of LPS on mRNA levels in HaCaT cells. (B)The effects of LPS on cell viability in HaCaT cells. (C) The effects of PREO on cell viability in LPS induced HaCaT cells. (D) The effects of PREO on cell viability in LPS-induced HaCaT cells Data are presented as percentages and blank was fixed at 100%. Values represent means ± standard error of the mean, n=3.

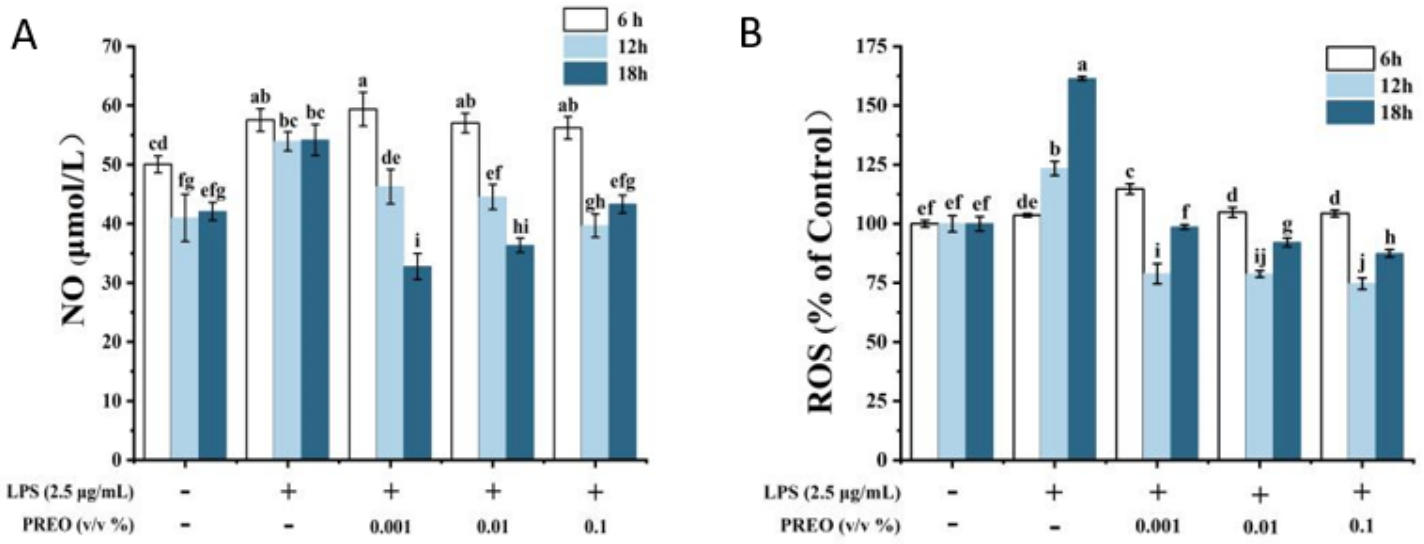

Figure 2

The effects of PREO on intracellular NO and ROS production in LPS-induced HaCaT cells. The HaCaT cells were treated with 2.5 μg/mL LPS for 20 h, then incubated with PREO for 6 h,12 h and 18 h. The cells were analyzed for nitrite production by the Griess method. Values represent means ± SD, n=3. p<0.01.

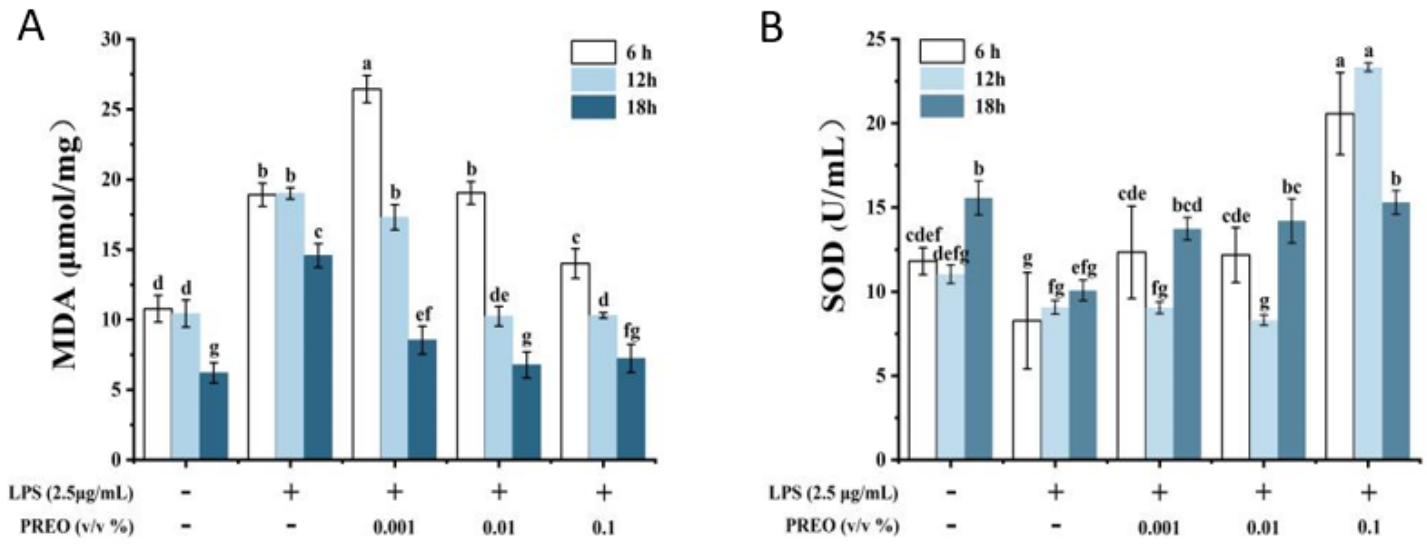

Figure 3

The effects of PREO on LPS-induced oxidative stress in HaCaT cells. The HaCaT cells were treated with 2.5 μg/mL LPS for 20 h, then incubated with PREO for 6 h,12 h and 18 h. The intracellular MDA and SOD levels were measured. Values represent means ± SD, n=3, p<0.01.

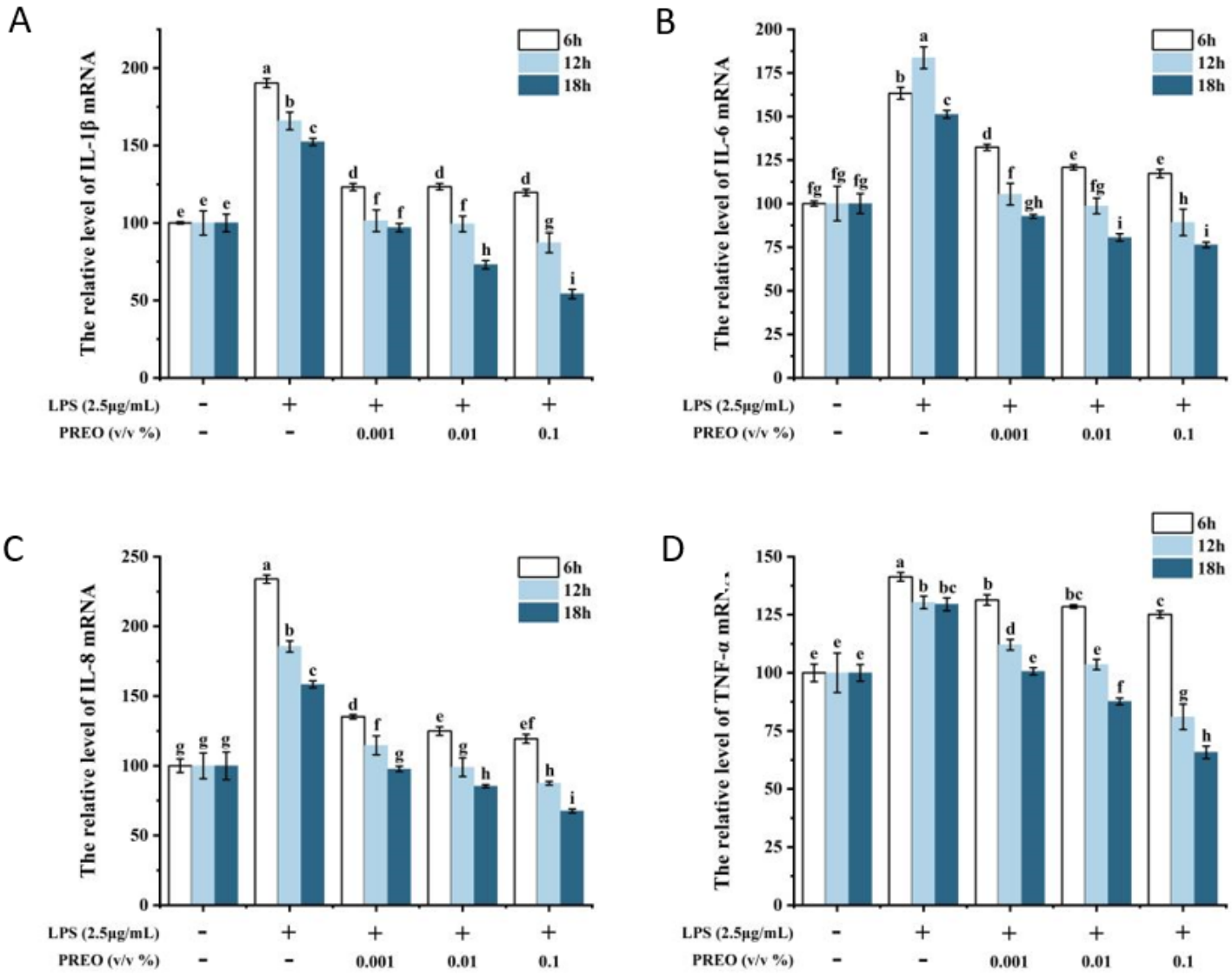

Figure 4

The effects of PREO on mRNA levels of proinflammtory cytokines expression in LPS-induced HaCaT cells. Cells were treated with 2.5 μg/mL LPS for 20 h, then incubated with PREO for 6 h,12 h and 18 h. The IL-1β, IL-6, IL-8 and TNF-α mRNA expression levels were measured using an RT-PCR analysis. Values represent means ± standard error of the mean, n=3. p<0.01.

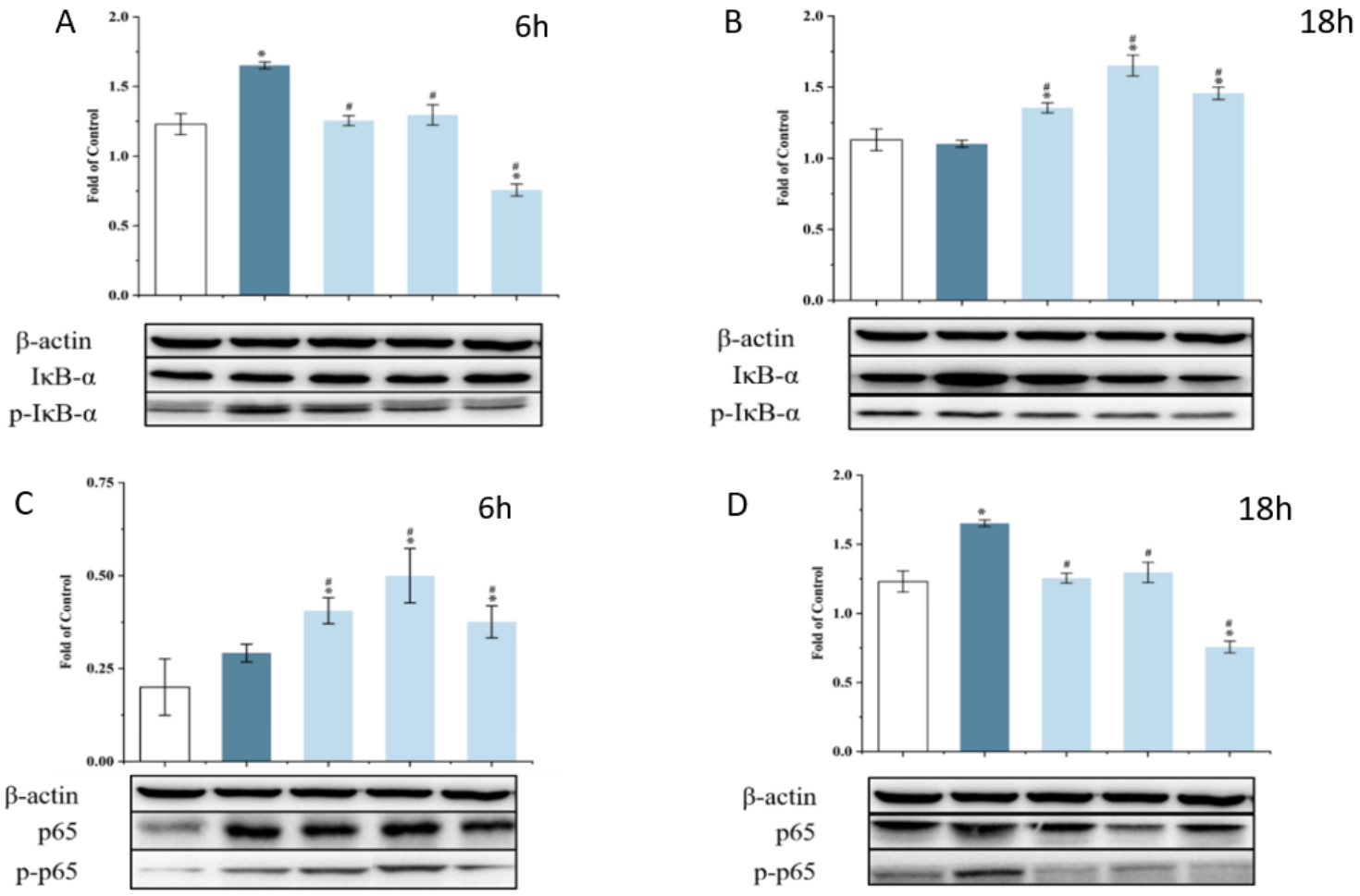

Figure 5

The effects of PREO on protein levels of proinflammtory cytokines IκB-α and p65 expressions in LPS-induced HaCaT cells. Cells were treated with 2.5 μg/mL LPS for 20 h, then incubated with PREO for 6 h and 18 h. A-B: IκB-alpha protein expression C-D: NF-kb p65 expression. Values represent means ± standard error of the mean. $p<0.01$.

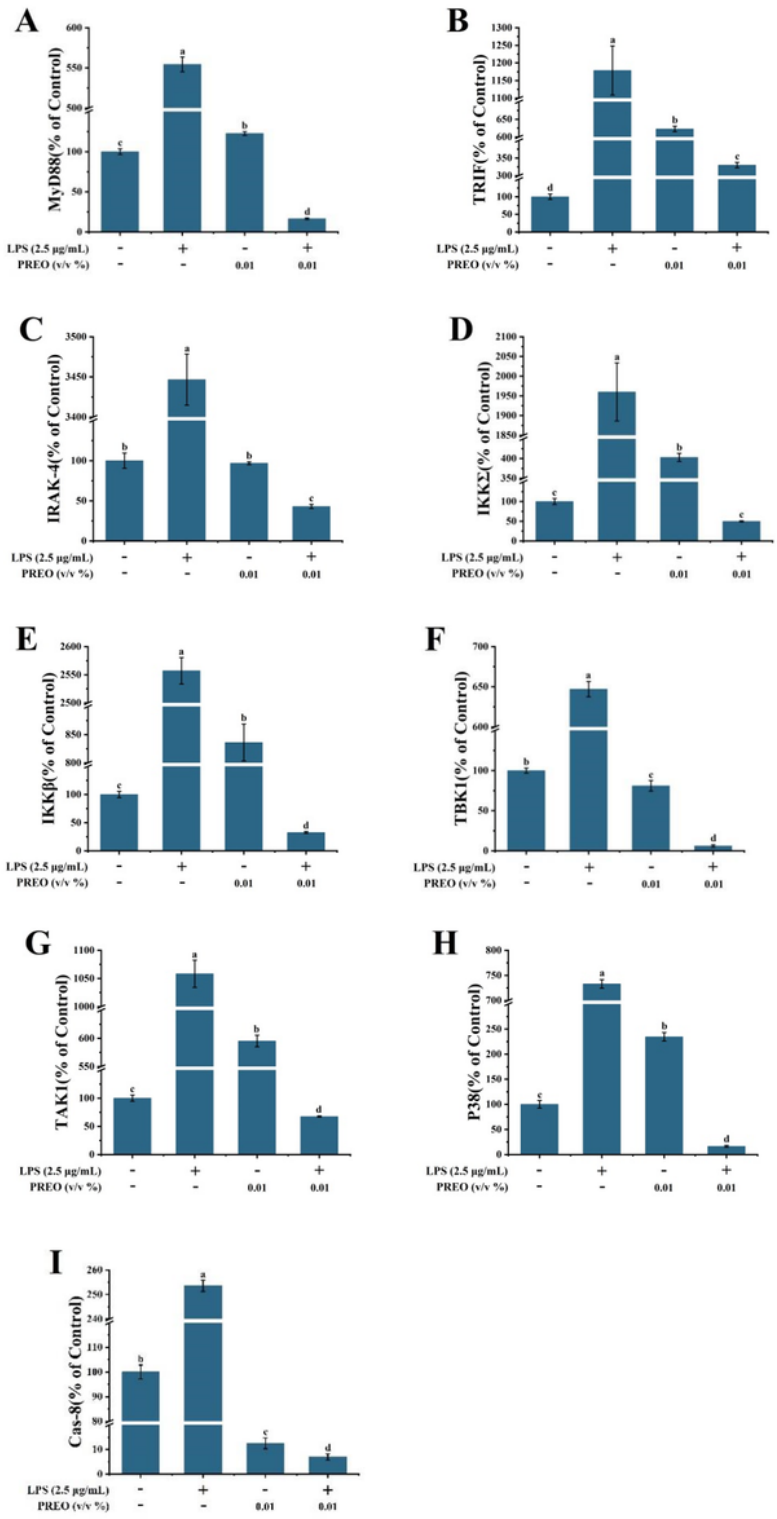

Figure 6

The effects of PREO on mRNA levels of TRL4 pathway in LPS-induced HaCaT cells. Cells were treated with 2.5 μg/mL LPS for 20 h, then incubated with PREO for 18 h. The MyD88, TBK1, Cas-8, TRAK-4, TAK1, IKKβ, IKKΣ, p38 and TRIF mRNA expression levels were measured using an RT-PCR analysis. Values represent means ± standard error of the mean, n=3. $p<0.05$.

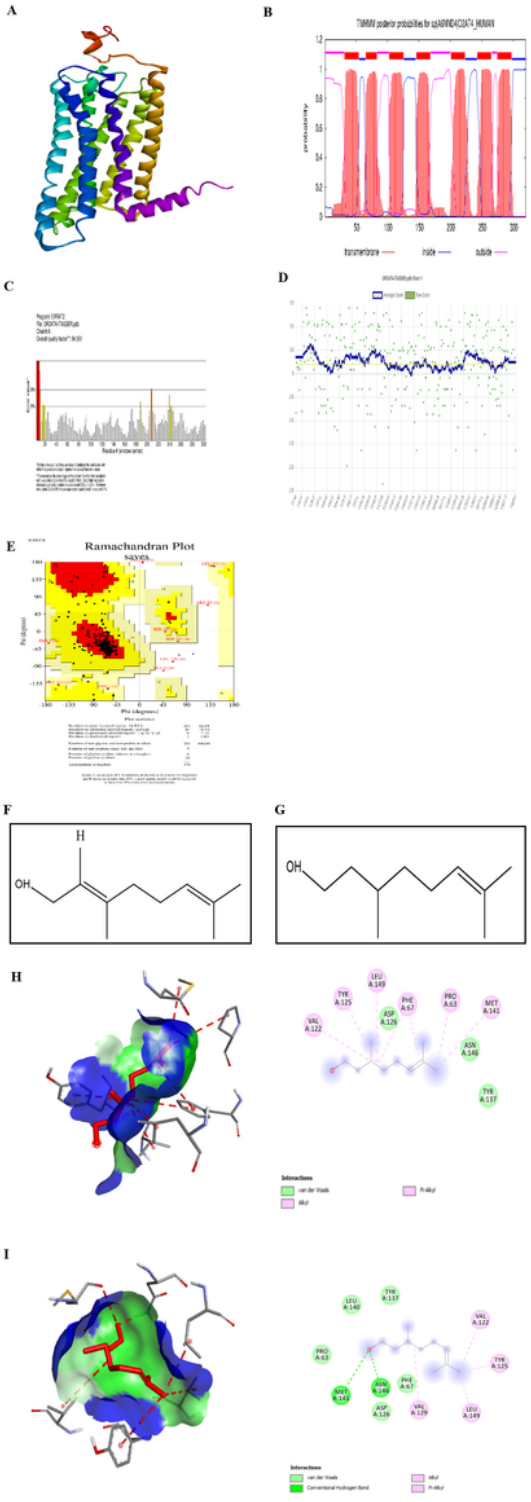

Figure 7

Molecular Docking. A: Protein structure of OR2AT4; B: TM regions of OR2AT4; C: Errat value; D: Verify3D; E: Ramachandran plot; F: Geraniol; G: Citronellol; H: Geraniol-OR2AT4 interaction; I: Citronellol-OR2AT4 interaction